Chemical Engineering Science 158 (2017) 108–116

Contents lists available at ScienceDirect

Chemical Engineering Science

journal homepage: www.elsevier.com/locate/ces

A kinetic inlet model for CFD simulation of large-scale bubble columns

Weibin Shi[a,b], Ning Yang[a,*], Xiaogang Yang[b]

[a] State Key Laboratory of Multiphase Complex Systems, Institute of Process Engineering, Chinese Academy of Sciences, P.O. Box 353, Beijing 100190, PR China

[b] International Doctoral Innovation Centre (IDIC), The University of Nottingham Ningbo, University Park, Ningbo 315100, PR China

ARTICLE INFO

Keywords:
CFD modelling
Bubble columns
DBS drag model
Gas distributor
New inlet model
Large-scale

ABSTRACT

For the simulation of industrial-scale bubble column reactors, while modelling the gas distributor as uniform inlets oversimplifies the inhomogeneity introduced by inlets, the direct simulation of the full geometry of gas distributor or sparger brings about enormous pre-processing work and huge computational cost. A new inlet model is therefore proposed in this paper to simplify the modelling of gas distributor and meanwhile maintain the simulation accuracy. The new inlet model is validated by the comparison of the model prediction with experiments and the CFD simulation incorporating the full geometry of gas distributor for bubble columns of small or large diameters. Comparisons of three different inlet boundary conditions, i.e., the direct simulation of gas distributor, the uniform inlet, and the new inlet model, are made in the simulation of the total gas holdup, the radial profiles of gas holdup at different cross-sections along the column height, and the axial velocity of liquid at various superficial gas velocities. The results indicate that the new inlet model is capable of achieving a good balance between simulation accuracy and computational cost for the CFD simulation of large-scale bubble column reactors.

1. Introduction

Bubble columns and their variants have been extensively utilized in chemical or process industries for gas-liquid or gas-liquid-solid reactions, such as oxidation, chlorination, alkylation, polymerization, hydrogenation, and fermentation. These reactors provide higher heat and mass transfer rates while maintaining lower operation and maintenance costs. For the design and scale-up of various processes, a large number of experimental studies have been carried out to investigate the hydrodynamics of gas-liquid flow in bubble columns at different operational parameters. However, these experimental studies (Deckwer, 1992) are usually carried out in lab-scale columns of diameters less than 0.5 m. Experiments on large-diameter columns are seldom reported due to the difficulty or complexity in experimental measurements. With the rapid development of computer technology and computational science in the past two decades, CFD is becoming a powerful tool in understanding the complexity of hydrodynamics. A number of studies have been conducted on various aspects of CFD simulation, e.g., the impact of turbulence models (Laborde-Boutet et al., 2009; Masood et al., 2014; Sokolichin and Eigenberger, 1999), drag forces (Li and Zhong, 2015; Xiao et al., 2013; Yang et al., 2011), lift forces (Lucas et al., 2016; Wang and Yao, 2016) and bubble breakage and coalescence models (Bordel et al., 2006; Chen et al., 2005b; Wang et al., 2006), and the coupling of CFD simulation with mass transfer (Bao et al., 2015; Wiemann and Mewes, 2005) or reaction kinetics (Rigopoulos and Jones, 2003; Troshko and Zdravistch, 2009; Van Baten and Krishna, 2004). Hitherto there are two main issues in CFD simulation of bubble columns. The first one is the sensitivity of simulation on closure models of interfacial momentum exchange, in particular, the drag force and other forces including lift or virtual mass force exerted by the surrounding liquid to the bubbles. There have been some studies regarding the effects of the lift coefficient C_L (Delnoij et al., 1997; Lucas et al., 2005; Lucas and Tomiyama, 2011; Sankaranarayanan and Sundaresan, 2002; Sokolichin et al., 2004; Tomiyama, 1998), and of the virtual mass force (Delnoij et al., 1997; Hunt et al., 1987). However, successful simulations have been reported in literature for either including lift and virtual mass forces (Deen et al., 2001; Rampure et al., 2007; Tabib et al., 2008; Zhang et al., 2006) or only using the drag force (Deen et al., 2000; Krishna and van Baten, 2001; Ranade and Tayalia, 2001). Actually the lift coefficient or lift force, as a result of pressure or velocity gradient, can generally be used to adjust the simulation of radial distribution of gas holdup, especially when the uniform inlet condition is applied. The physical basis of these non-drag forces still requires further investigation. In this study we temporarily isolate these effects from that of drag force and inlet conditions. The second issue is the

* Corresponding author.
E-mail address: nyang@ipe.ac.cn (N. Yang).

http://dx.doi.org/10.1016/j.ces.2016.10.005
Received 11 April 2016; Received in revised form 29 September 2016; Accepted 6 October 2016
Available online 07 October 2016

Nomenclature

C_D	effective drag coefficient for a bubble around a swarm, dimensionless
d_b	bubble diameter, m
U_g	superficial gas velocity, m/s
U_l	superficial liquid velocity, m/s
u	velocity vector, m/s
k	turbulent kinetic energy, m^2/s^2
g	gravity acceleration, m/s^2
H	distance from the bottom surface, m
F^D	drag force, N/m^3
t	time, s
P_T	total pressure, MPa
P_S	vapour pressure of the liquid, MPa
D_C	column diameter, m
X^W	weight fraction of the primary liquid in the mixture, w/w

Greek letters

α	phase volume fraction, gas holdup
ε	turbulence dissipation rate
μ	molecular dynamic viscosity, Pa s
μ_t	turbulence dynamic viscosity, Pa s
ρ	fluid density, kg/m^3
σ	surface tension, N/s
Γ	gas distributor parameter

Abbreviations

DBS	double-bubble-size
EMMS	energy-minimization multi-scale
CARPT	Computer-automated radioactive particle tracking
CT	Computed tomography

Subscripts

g	gas
l	liquid

simplification of gas distributor or sparger as a uniform inlet or the high computational cost arising from the direct modelling of the full geometry of gas distributors. The latter issue is less covered in literature but still a challenge for the simulation of industrial-scale columns.

Gas distributors or spargers are reported to have great influence on flow behaviours. Hills (1974) and Camarasa et al. (1999) showed that the gas holdup, liquid velocity, bubble size and bubble velocity altered significantly when using different gas distributors, e.g., the sieve plates of various configurations, the porous plates, the multi- or single- orifice nozzles. Mudde et al. (2009) presented a densely arranged multi-needle sparger to obtain a uniform bubble injection, and found that the homogeneous flow regime was extended up to a gas fraction of 55%. Haque et al. (1986) reported that the mixing time and total gas holdup were significantly affected by sparger designs. Moreover, Dhotre and Joshi (2007) stated that the distributor of different configurations generated the initial bubbles of a certain size and gas holdup, which in turn influenced the overall flow pattern. Some researchers have studied the effect of distributors by using CFD modelling. Ranade and Tayalia (2001) modelled a shallow bubble column of single- or double-ring spargers, and the simulation indicated that the fluid dynamics and mixing in shallow bubble column reactors were controlled by sparger configuration. Akhtar et al. (2006) simulated the perforated plates with different open areas, indicating that including the real gas distributors in simulation can lead to asymmetric flow patterns which were otherwise smoothened when a uniform gas source was used in CFD simulation. Dhotre and Joshi (2007) studied the influence of the size, location, opening area and hole diameter of nozzles on the flow pattern of CFD simulation. They analysed the flow pattern within the gas chamber under the distributor and velocities through all the holes, and found that the chamber configurations affected the uniformity of gas distribution in the sparger region of bubble columns. It appears that an interaction exists between the chamber and sparger, which may affect the stability of the plume. Bahadori and Rahimi (2007) investigated the influence of the number of orifices on gas hold-up and liquid phase velocity by CFD modelling. They reported that increasing the number of orifices in the sparger increased the total gas holdup in a shallow bubble column and each local orifice contributed to liquid circulation and mixing. Li et al. (2009) reported that the distributor configurations had strong impact on the asymmetric flow and mixing characteristics in the vicinity of gas distributor. Rampure et al. (2009) included the plenum area under the gas distributor into the CFD simulation. They modelled the perforated plate as a porous zone and adopted empirical correlations to obtain the model input parameters. Compared to the cases using uniform inlet conditions or directly modelling the gas distributors, the purpose of this study is to develop a new kinetic inlet model which could equivalently reflect the kinetic information of gas velocity gradient and the inhomogeneity introduced through the inlet, without the need to directly model the real inlet geometry. It may provide a simpler way without the necessity to simulate the perforated plate as well as the gas chamber underneath, while the simulation accuracy is still guaranteed.

Direct modelling of the full geometry of gas distributor or specifying the mass sources at the real positions of holes has been reported in literature (Tabib et al., 2008; Ziegenhein et al., 2013). However, this may also lead to a significant increase in pre-processing work, grid number and complexity as well as computational cost. For example, when the number of holes in a gas distributor is around 60 and the hole diameter is larger than 2 mm, it is possible to include every single hole in the simulation of lab-scale bubble columns. Nevertheless, the gas distributors used in industrial-scale columns are far more complicated, involving hundreds of holes with the size around 1 mm. Chen et al. (2005a) used 0.7 mm- or 1.32 mm-diameter holes on perforated plate and stated that it was impossible to include the gas distributor into the simulation due to the fact that the direct modelling of gas distributor would require millions of cells. The computational cost would become unaffordable if more complicated geometries (e.g., heat exchange tubes or internals) need to be investigated, or more transport equations need to be solved, e.g., the three-fluid model for gas, liquid and solid phases, or the population balance equations for bubble coalescence and break-up, or species transport equations to incorporate mass transfer and reaction kinetics.

Some previous CFD studies attempted to simplify the gas distributor as a uniform inlet across the whole bottom surface since this may greatly reduce the number of grids and computational cost. However, this simplification may cause some under-prediction of gas holdup for large diameter columns, which will be further elucidated in this study. Therefore, as a compromise of these two methods, the objective of this work is to propose a new inlet model which is able to reflect the non-uniformity of the gas inlet and achieve the reasonable simulation and meanwhile reduce the computational cost. Section 2 will present the computational models to be used in the simulations and demonstrate the new inlet model. Numerical details in CFD simulations conducted in this work will be given in Section 3. Section 4 provides the

simulations utilizing the new inlet model in small- and large-diameter columns. The simulation validates the new model function, demonstrating its capability to achieve the balance between simulation accuracy and computational cost in CFD simulation of large-scale bubble column reactors.

2. Mathematical formulation

2.1. Computational models

The equations of Eulerian-Eulerian approach used in this work are given as below, consisting of mass and momentum balance equations to describe the hydrodynamics of the continuous liquid or disperse gas phases:

$$\frac{\partial(\alpha_k\rho_k)}{\partial t} + \nabla\cdot(\alpha_k\rho_k\vec{u_k}) = 0\ (k = \text{liquid or gas}) \tag{1}$$

$$\frac{\partial(\alpha_k\rho_k\vec{u_k})}{\partial t} + \nabla\cdot(\alpha_k\rho_k\vec{u_k}\vec{u_k}) = -\alpha_k\nabla P + \nabla\cdot\bar{\bar{\tau}}_k + \alpha_k\rho_k g + F_k^D \tag{2}$$

Closure laws are required for the phase interaction forces. In this study, only the drag force is employed as it is considered to be the predominant interfacial force in gas-liquid flows in bubble columns (Laborde-Boutet et al., 2009; Larachi et al., 2006). The drag force is formulated as:

$$F_g^D = -F_l^D = \frac{3}{4}\alpha_g\frac{C_D}{d_b}\rho_l|\vec{u_g} - \vec{u_l}|(\vec{u_g} - \vec{u_l}) \tag{3}$$

In the equation above, C_D/d_b is a critical lumped parameter in CFD simulation. It can be either calculated from several correlations in literature, or be derived from the DBS drag model (Yang, 2012; Yang et al., 2011). The DBS model extended the energy minimization multi-scale (EMMS) approach for gas-solid fluidization to gas-liquid flows, and its physical background and further details can be found in the previous publications (Chen et al., 2009; Xiao et al., 2013; Yang, 2012; Yang et al., 2007, 2011). The lumped ratio was formulated by Xiao et al. (2013) as:

$$C_D/d_b = \begin{cases} 431.14 - 6729.02U_g + 35092.2U_g^2, & U_g \le 0.101\ m\cdot s^{-1} \\ 122.49 - 553.94U_g + 741.24U_g^2, & U_g > 0.101\ m\cdot s^{-1} \end{cases} \tag{4}$$

The standard k-ε model for the two-phase mixture is employed as given below:

$$\frac{\partial}{\partial t}(\rho_m k) + \nabla\cdot(\rho_m\vec{u}_m k) = \nabla\cdot\left(\frac{\mu_{t,m}}{\sigma_k}\nabla k\right) + G_{k,m} - \rho_m\varepsilon \tag{5}$$

$$\frac{\partial}{\partial t}(\rho_m\varepsilon) + \nabla\cdot(\rho_m\vec{u}_m\varepsilon) = \nabla\cdot\left(\frac{\mu_{t,m}}{\sigma_\varepsilon}\nabla\varepsilon\right) + \frac{\varepsilon}{k}(C_{1\varepsilon}G_{k,m} - C_{2\varepsilon}\rho_m\varepsilon) \tag{6}$$

2.2. A new inlet model

As mentioned in the introduction section, the CFD modelling of large-scale bubble columns by employing the actual geometry of gas distributor may impose an insurmountable difficulty due to the constraint of mesh generation and computational cost. It would be desired and practical if a kinetic model could be introduced to incorporate the flow behaviour but avoid modelling the actual geometry of gas distributor. A new inlet model is proposed here to account for the effect of entrance velocity gradient with an attractive benefit of significant reduction of the number of mesh cells. This model attempts to take the number and size of the perforated holes into consideration for a particular type of gas distributor, i.e., the perforated plates. For this type of distributor, the gas flows through each perforated hole to form jet arrays, generating a velocity fluctuation around the holes along the radial direction due to the entrainment of the carrier fluid. Although these local jet flows may not essentially affect the hydrodynamic behaviours if the height to dimension ratio H/D is larger enough, there can be a very strong influence on the flow pattern in the non-fully-developed region. Moreover, Guan et al. (2015) reported that the flow pattern in bubble columns with internal tubes was always not fully developed due to the existence of internal tube banks. In this case, the inlet condition may play important roles.

Behkish et al. (2006) proposed a correlation of gas holdup in bubble columns or slurry bubble columns based on 3881 experimental data points. The model parameters included the pressure, temperature, gas superficial velocity, solid concentration, particle density/concentration, reactor size, and gas sparger characteristics. Rearranging the correlation of Behkish et al. (2006) leads to

$$\tilde{u}_s = 2.24\times10^2\times\alpha^{1.8}\times\left(\frac{\mu_L^{0.313}\sigma_L^{0.486}}{\rho_L^{0.747}\rho_G^{0.319}}\right)\times\left(\frac{P_T - P_S}{P_T}\right)^{0.365}\times\left(\frac{D_C}{D_C+1}\right)^{0.211}\times\Gamma^{-0.095}\times e^{0.436X_W} \tag{7}$$

where u_s is the superficial gas velocity, α is the gas holdup, and Γ represents the gas distributor parameter. Other parameters are either the physical properties or operational parameters. The local gas holdup is a function of radial position and can be correlated by an exponential function of radial position, as will be demonstrated in Eq. (14) in the following sections. Hence if we apply Eq. (7) to the local radial positions, it can be deduced that the local gas velocity could also be expressed as an exponential function of radial position. In general, the fluctuating trend and magnitude of local jet flows could be averaged and approximated by a normal distribution-like function which defines the local gas velocity at a given point on the inlet boundary. Thus, it may be reasonable to assume that the entrance velocity for the gas distributor could be approximated by the exponential function. Based on this consideration, we thus propose the simplified inlet model. It should be pointed out that this approximate approach should be distinguished from the method of modelling the real holes. The new inlet model for a perforated plate could then be formulated as:

$$\tilde{u}_s = \begin{cases} (1.5 + \frac{\Gamma}{100})U_g\cdot e^{\frac{-r^2}{b}}, & Ug \le 0.12m/s \\ (0.75 + \frac{\Gamma}{100})U_g\cdot e^{\frac{-r^2}{b}}, & Ug > 0.12m/s \end{cases} \tag{8}$$

which is also subject to the continuity function:

$$Q = \sum\frac{\pi}{4}d_i^2\cdot u_i = \frac{\pi}{4}D^2\cdot U_g = \int_0^R \tilde{u}_s\cdot 2\pi r dr \tag{9}$$

Table 1
Parameters of 5 typical perforated plates.

Configuration	Hole number	Do (mm)	Dc (m)	do/Dc	ζ	Γ	Umax (m/s)	b
1	61	0.4	0.14	0.0029	0.0498	72.8416	0.2228	0.0026
2	121	1.32	0.14	0.0094	1.0757	23.6553	0.1737	0.0038
3	225	1.32	0.19	0.0069	1.086	43.9871	0.1940	0.0060
4	241	3	0.45	0.0067	1.0711	59.9278	0.2099	0.0280
5	301	0.77	0.45	0.0017	0.0881	46.7722	0.1968	0.0326

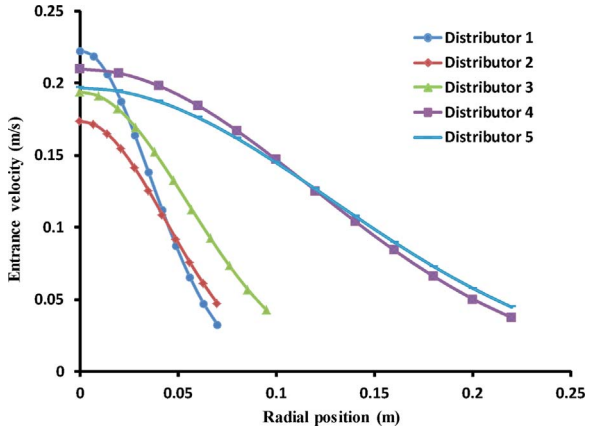

Fig. 1. Inlet gas velocity profile for different geometrical parameters (Ug=0.1 m/s).

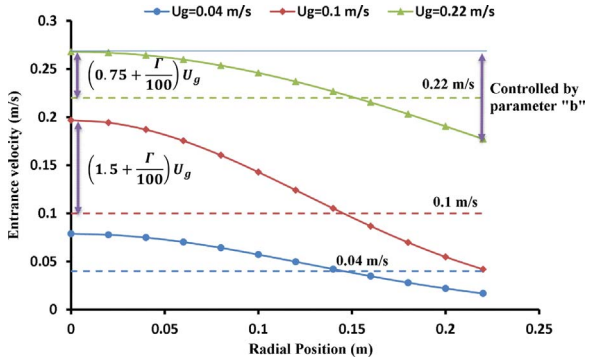

Fig. 2. Inlet gas velocity profile for Distributor 5 (Ug=0.04, 0.1, 0.22 m/s).

where d_i and u_i are the diameter and the through hole velocity of i-th inlet hole respectively, r is the non-dimensional radial position, and the parameter b can be determined by solving the continuity function Eq. (9). Γ is a lumped coefficient representing the influence of gas distributor configurations and defined by Behkish et al. (2006) as:

$$\Gamma = K_d \times N_O d_O^{\alpha} \tag{10}$$

$K_d$is the distributor coefficient that equals 1.364 for perforated plates, N_O is the number of orifice holes on the plate, and d_O is the diameter of orifice holes. The index α depends on the value of ζ, the free area of the distributor:

$$\zeta = N_O\left(\frac{d_O}{D_C}\right)^2 \times 100 \tag{11}$$

For perforated plates,
α = 0. 017, when ζ<0.055;.
α = 0. 303, when0. 055 ≤ ζ≤0.3;.
α = 0. 293, when ζ>0.3.

Table 1 lists the distributor parameters for five typical perforated plates. The gas velocity distribution at the inlet is illustrated in Fig. 1 for five different gas distributors at U_g=0.1 m/s, and Fig. 2 shows the velocity profile of distributor 5 at different superficial velocities.

It should be pointed out that an exact inlet model could also be correlated from the CFD simulation of the actual configuration including the gas plenum chamber and the gas distributor with consideration of the liquid height above the gas distributor, such as the work of Rampure et al. (2009). However, Dhotre and Joshi (2007) reported that the gas velocity profile at the holes was not only dependent on the superficial velocity and the number and diameter of orifice holes, but also on the pressure drop of distributor and liquid bulk phase as well as the chamber geometry. Actually an exact simulation of the velocity profile around holes also requires the inclusion of the two-phase flow above the distributor or even an iteration process between the gas chamber and the bulk region of two-phase flow, which is far more complicated and beyond the scope of this study. Here we propose a simplified function to replace the inlet velocity distribution which is only a function of distributor geometry and superficial gas velocity for engineering application.

For these five perforated plates with different geometrical configurations in Fig. 1, the maximum at the centre of the column are approximately twice the superficial velocity according to the Hagen-Poiseuille's Law. The effects of model parameters are illustrated in Fig. 2. The maximum value is determined by geometrical parameters, i.e., the ratio (0.75 + Γ/100) or (1.5 + Γ/100). The slopes of the curve are dependent on the parameter b which can be obtained by solving the continuity function. We may assume that the flow near the distributor region could be approximated by a free-stream flow in a pipe. When the flow rate is relatively lower (0.04–0.1 m/s), the pressure loss is linear with the velocity so that the steepness of the profiles increases. According to Law of Blasius, the sum of viscous shear stress and turbulent stress τ_w can be expressed as $\tau_w = 0.03325\rho U^{7/4}(\upsilon/R)^{1/4}$. Hence when the flow enters the fully-developed heterogeneous (churn-turbulent) regime ($U_g > 0.12$ m/s), the velocity profiles in the cross-sections close to the entrance of bubble columns tend to be flat and the velocity gradient is restricted to the near wall region.

It should also be pointed out that the new inlet model proposed here has only been tested for perforated plates in which holes are uniformly distributed at the whole cross-section in concentric circles or in a triangular pitch, with the size of holes not exceeding 4 mm and the number of holes more than 60. Although further validation is required, the proposed model is potentially capable of representing distributor configurations beyond this range or other types of gas distributors such as porous plates or multiple-orifice nozzles.

3. Simulation details

To validate the effect of the new inlet model, simulations have been carried out for the air-water bubble columns of Hills (1974). The detail information is listed in Table 2.

The average size of cells is about 7 mm for the case of Grid 1 (Fig. 3) which is equivalent to 14(r)×36(θ)×150(z) nodes and results in approximately sixty thousand cells in total. The grid sensitivity was further tested in the two stages with a grid refinement of a factor of about 1.3 in all directions. Grid 2 generates twice the total number of cells of Grid 1, and Grid 3 doubles the total number of cells of Grid 2 in a similar manner.

3D pressure-based solver of Ansys Fluent® is used in this work. The time step is set to be 0.0005 s in the beginning. When the physical time reaches 10 s, the time step increases to 0.001 s till the flow time reaches 30 s, and then the time step is fixed to be 0.005 s. The quasi-steady state is considered to be achieved after 80 s. Data sampling statistics for the next 80 s is considered to be sufficient to illustrate the time-averaged characteristics of the flow fields. The new inlet model is

Table 2
Details of experimental setup in Hills (1974).

Column Diameter (m)	Column Height (m)	Observation Height (m)	No. of holes on distributor	Diameter of holes (mm)	ζ	Superficial gas velocity (m/s)
0.138	1.37	0.6	61	0.4	0.0498	0.038–0.127

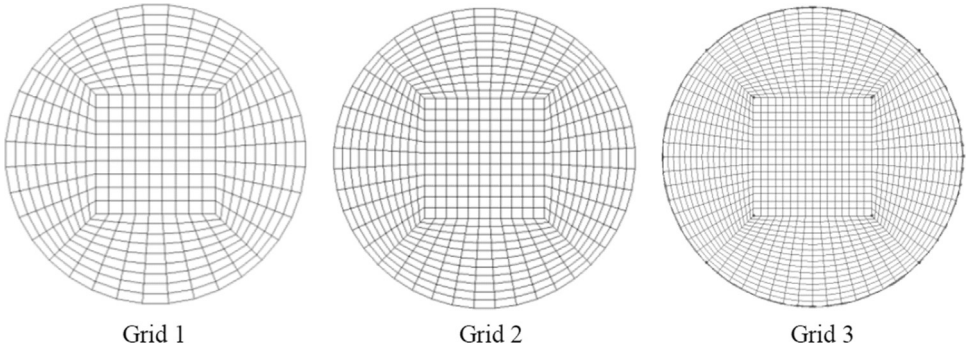

Fig. 3. Mesh set-up at bottom surface.

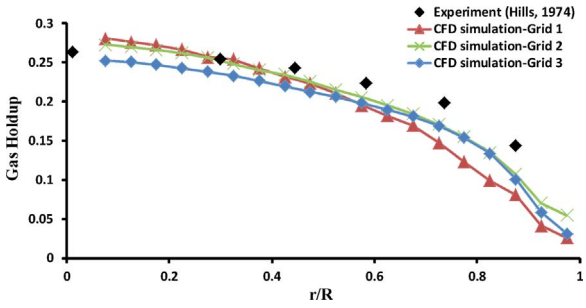

Fig. 4. Comparison of simulated gas holdup profile with three different grids (Ug=0.064 m/s).

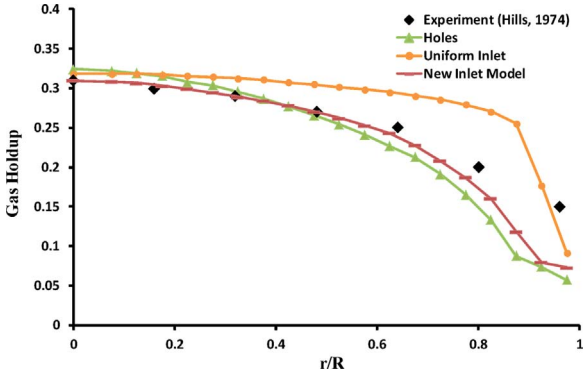

Fig. 5. Radial distribution of gas holdup using different inlet conditions (Ug=0.095 m/s, H=0.6 m, H/D=4.35).

integrated into the user define function (UDF). The volume fraction of gas phase is set to be 1 at inlet. The outlet boundary is set as a pressure outlet at the top. Non-slip conditions are applied for both liquid and gas phases at the vessel wall. A grid sensitivity test has been conducted for Grid 1, Grid 2 and Grid 3, and they can yield quantitatively the similar results (Fig. 4), and Grid 2 is used in the succeeding simulations to investigate the effects of inlet models.

4. Results and discussion

4.1. Validation of the new inlet model

Three cases for different superficial gas velocities are simulated for the Hills system: 0.038, 0.095 and 0.127 m/s, representing the homogenous, transitional, or heterogeneous regimes respectively. The prediction of gas holdup distribution by using the new inlet model is compared with experimental data of Hills (1974) and the simulation of Yang et al. (2011) and Xiao et al. (2013) in which all the gas inlet holes were included.

Fig. 5 compares the time-averaged gas holdup distribution for three different inlet models at superficial gas velocity Ug=0.095 m/s. “Holes”

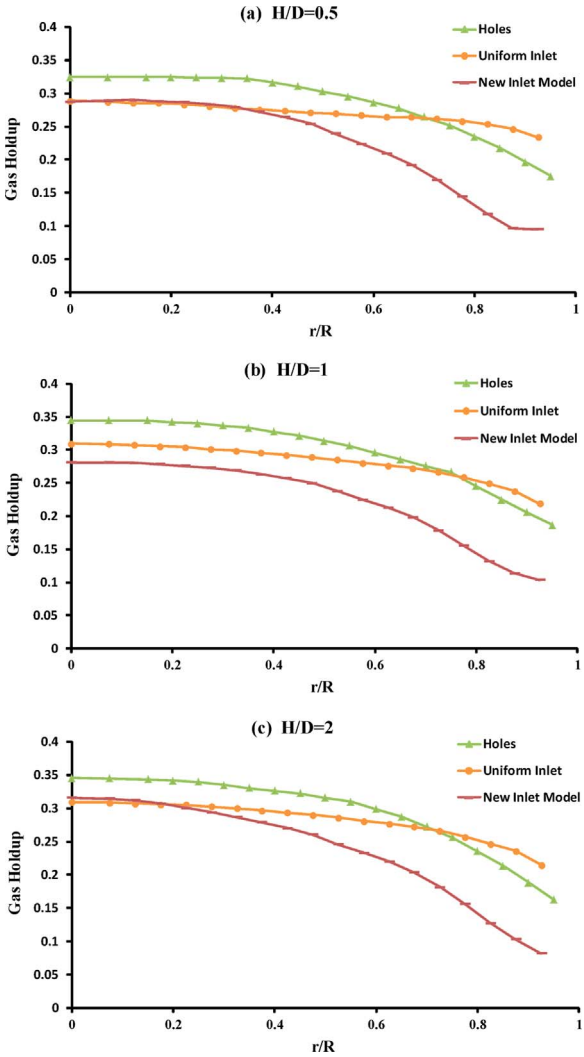

Fig. 6. Gas holdup radial distribution along the column height (from the top to bottom: H/D=0.5, 1, 2; Ug=0.095 m/s).

means that all the orifices at the gas distributor are modelled so that the gas is introduced through each orifice holes. “Uniform Inlet” means that the distributor geometry is not modelled and the gas is introduced uniformly through the whole bottom surface of the column. “New Inlet Model” denotes that the gas is introduced through the profile functions of the new inlet model. Although all the three inlet models achieved reasonable agreements with experimental data, it can be seen that the gas holdup distribution curve tends to be flat for the “Uniform Inlet” case whereas the other two fit the experimental data better.

Fig. 6 presents the evolution of gas holdup profiles along the

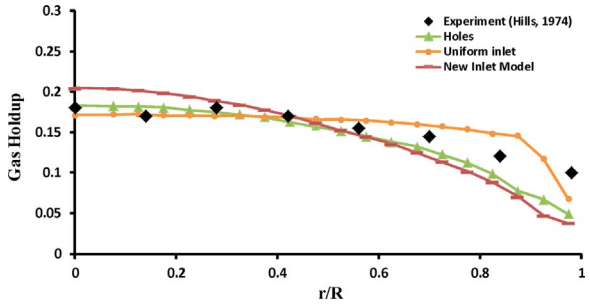

Fig. 7. Radial distribution of gas holdup using different inlet conditions (Ug=0.038 m/s, H=0.6 m).

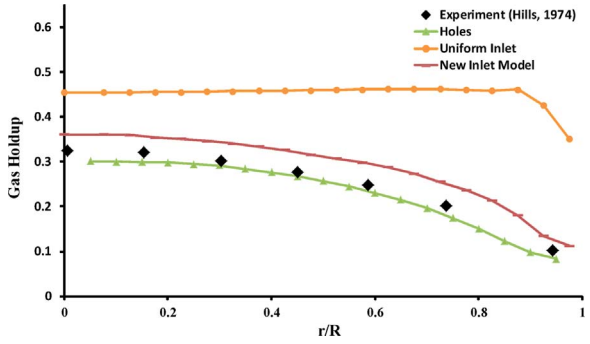

Fig. 8. Radial distribution of gas holdup using different inlet conditions (Ug=0.127 m/s, H=0.6 m).

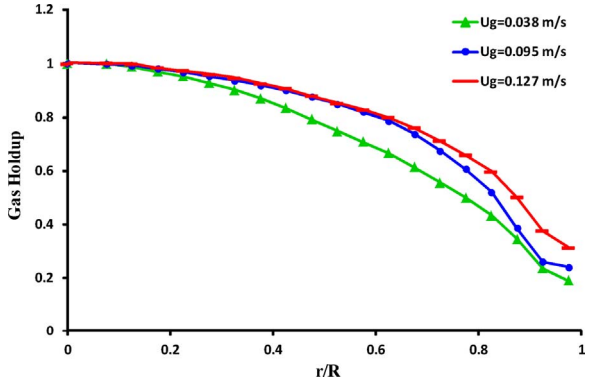

Fig. 9. Radial distribution of normalized gas holdup profile using new inlet model (H=0.6 m).

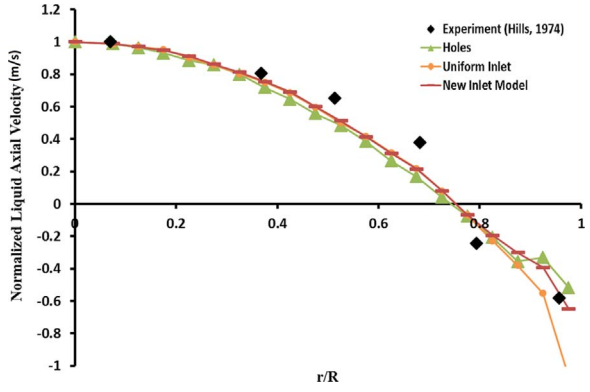

Fig. 10. Radial distribution of normalized axial liquid velocity (Ug=0.95 m/s, H=0.6 m).

column height for the three gas inlet conditions. Since the experimental data of lower H/D ratios is not available, only the simulation results are plotted in the figure. For the "Holes" case, the gas holdup turns out to be a monotonous parabolic profile when H/D=0.5. This reflects the

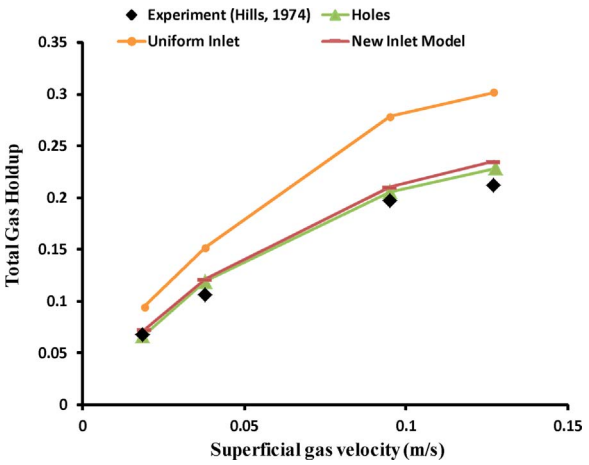

Fig. 11. Comparison of simulated total gas holdup profiles with experiments of Hills (1974).

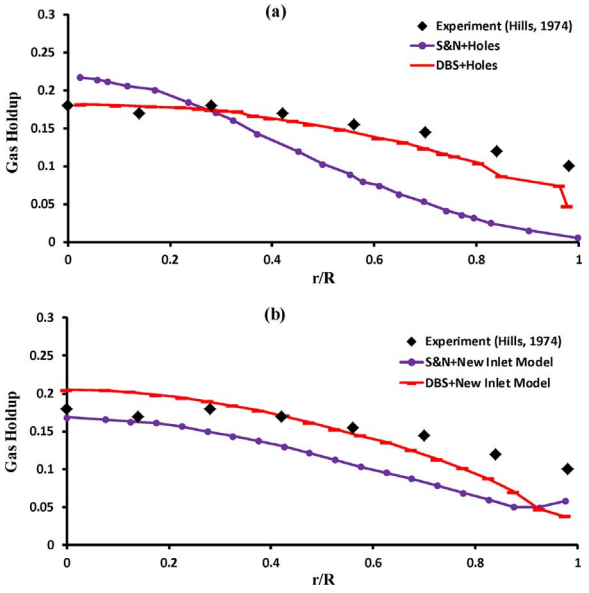

Fig. 12. Radial distribution of gas holdup using different drag models in combined with (a) Holes model; (b) New Inlet Model (Ug=0.038 m/s, H=1.32 m).

influence of gas momentum distribution formed by the orifice holes on the sparger. The parabolic profile holds coherently and even rises slightly as a whole with increasing the H/D ratio. On the one hand, for the uniform inlet condition, it allows the gas to be introduced from the entire bottom surface, and the gas holdup profile is shown to be consistently flat at all cross-sections, showing the uniform momentum distribution. On the other hand, the performance of new inlet model is between the "Holes" and "Uniform Inlet" cases. For the new inlet model, it captures the performance of the "Holes" case to some extent, especially the pattern of inlet gas momentum distribution and the resulting parabolic shape of gas holdup profile, even though the absolute magnitudes are not exactly the same. The reason for the difference is that the direct simulation of holes on the sparger actually introduces much higher gas injection velocity at each inlet hole and consequently affects the sparging region. However, the difference becomes smaller for higher H/D, as shown in Fig. 5 (H=0.6 m, H/D=4.35).

The simulations in Figs. 5 and 6 also indicate that, for the new inlet model, the difference in radial profiles for H/D=2 (Fig. 6c) and H/D =4.35 (Fig. 5) is smaller. This implies that the influence of the inlet condition (or gas distributor) is marginal for higher H/D, and the evolution of radial distribution along the height does not change

Table 3
Bubble column parameters of Chen et al. (1999).

Column Diameter (m)	Column Height (m)	Observation Height (m)	No. of holes on distributor	Diameter of holes (mm)	ζ	Superficial gas velocity (m/s)
0.44	2.43	1.32	301	0.7	0.076	0.1

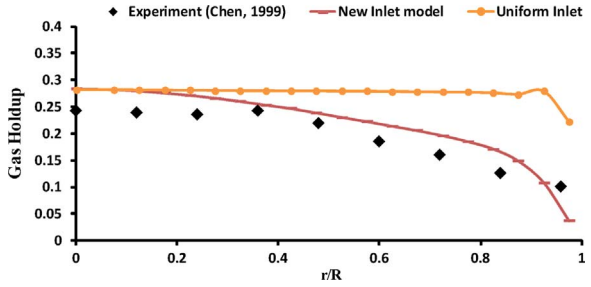

Fig. 13. Radial profile of gas holdup in comparison with the CT data of Chen et al. (1999) (Ug=0.1 m/s, D=0.44 m).

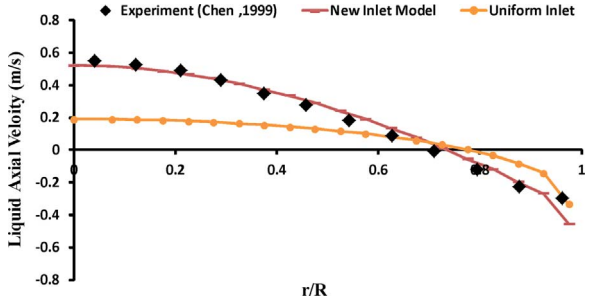

Fig. 14. Radial profile of liquid axial velocity in comparison with the CARPT data of Chen et al. (1999) (Ug=0.1 m/s, D=0.44 m).

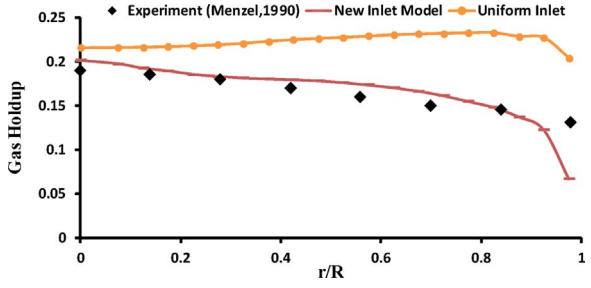

Fig. 15. Radial profile of gas holdup in comparison with the experiment of Menzel et al. (1990) (Ug=0.072 m/s, D=0.6 m).

noticeably for each specific distributor.

Figs. 7 and 8 present the radial distribution of gas holdup at Ug=0.038 m/s and Ug=0.127 m/s respectively. The results indicate that the uniform inlet overestimates the gas holdup at higher gas flow rate. While the "Holes" model performs the best, the new inlet model can also yield reasonable simulation. It should be pointed out that some previous studies have used the uniform inlet condition and also obtained good simulation results. This issue is complicated and, to our knowledge, it is related to two aspects. Firstly, the performance of uniform inlet is problem-dependent and a critical evaluation is still lacking on the simulation of different operating conditions and column geometries. Secondly, the simulation is also pertinent to the models of drag force or non-drag forces such as lift and virtual mass force. Some studies involved the lift force for the cases of the uniform inlet conditions, and hence the radial profile of gas holdup becomes parabolic. However, the simulation is also sensitive to the choice of lift coefficient. This article only focuses on the inlet conditions and the effects of non-drag forces have been omitted. We cautiously point out that the interaction between inlet conditions and physical models may be important, but has not yet been analysed or reported in literature.

Although the simulation of the new inlet model in Figs. 7 and 8 did not perfectly fit the experimental data, acceptable agreement is achieved with the error less than 20% for the majority part of the curves. The new inlet model reasonably allocates the gas momentum onto the cross-section at the bottom by the distribution profile functions, and hence the prediction can qualitatively capture the main characteristics of the experiments and the "Holes" case.

Fig. 9 presents the gas holdup profile normalized by the centreline values at three different superficial gas velocities (Ug=0.038, 0.095 and 0.127 m/s). It can be seen that the three profiles of gas holdup bear some analogy. In this case, it is reasonable to establish the following equation for gas holdup:

$$\frac{\partial \alpha}{\partial t} + \vec{u}\cdot\nabla\alpha = D\nabla^2\alpha \tag{12}$$

.

The first term vanishes in the fully developed region, and hence in radial direction

$$u_r\cdot\frac{\partial \alpha}{\partial r} = D\frac{\partial}{\partial r}\left(\frac{\partial \alpha}{\partial r}\right) \tag{13}$$

By solving Eq. (13), we obtain:

$$\frac{\partial \alpha}{\partial r} = C\cdot e^{\frac{u_r}{D}r} \tag{14}$$

where C and D are coefficients. Eq. (14) indicates that the gas holdup gradient in radial direction can be expressed in the form of an exponential function. It is reasonable to deduce that the similar expression holds for the inlet condition.

Fig. 10 shows the profile of normalized axial liquid velocity (relative to the centreline liquid velocity) along the radial direction. The normalized axial liquid velocity profiles are very similar and all of them are close to the experiment results, indicating that inlet conditions do not affect the flow pattern of liquid-phase. However, it should be pointed out that the simulated absolute centreline liquid velocities with all the inlet conditions are lower than experiments. This may be relevant to the simplified treatments for holes of sparger. For the "Holes" case, the hole diameter of the distributor was enlarged from 0.4 to 2 mm while maintaining the original number of holes in order to decrease the mesh number and mesh skewness. Therefore, the gas velocity at holes is actually lower than that of real cases, which may lead to the underestimation of liquid axial centreline velocity. The simulation is similar to the results of Yang et al. (2011).

Fig. 11 compares the simulated total gas holdup and the experiments for three different gas inlet models. The uniform inlet overestimates the total gas holdup especially at higher superficial gas velocities, whereas the other two models give good simulation. In the "Holes" case, the increase of gas holdup slows down with increasing superficial gas velocity. In the meantime, unlike the uniform inlet case, the new inlet model does not change this dampening tendency and can achieve similar effect that can only be obtained by the multi-hole inlet boundary. In conjunction with the DBS drag model, the new inlet model shows great adaptability for the prediction of both the total and the radial distribution of gas holdup without the need of adjusting modelling parameters.

It can be inferred from Figs. 5–11 that, on one hand, including

exactly the real number and size of holes into the simulation is necessary to acquire accurate prediction for all the three superficial velocities, but this requires approximately 700,000 cells for a lab-scale hollow bubble column. On the other hand, utilizing the new inlet model as an approximation can achieve acceptable agreements with experimental data in all the three cases, and the total cell number is reduced to approximately 60,000. The computational cost was apparently reduced to a great extent (approximately one tenth of the "Holes" case) without much sacrifice of the simulation accuracy. This may be of more significance for pilot- or industrial-scale bubble column reactors in which a large number of internals of complex geometry may reside, and in such cases the total number of cells could easily soar up to as many as tens of millions or even hundreds of millions. The new inlet model greatly reduces the grid number and unbearable computational cost by orders-of-magnitude.

It should be pointed out that the drag model is the predominant factor for the accuracy of simulation compared to the inlet boundary conditions. For example, the Schiller-Naumann (S & N) drag model still largely under-predicts the gas holdup, even if the "Holes" model or the new inlet model is employed, as shown in Fig.12. For the two different inlet boundary conditions, the DBS drag model consistently shows the better agreement with the experiments than the Schiller-Naumann drag model, which was also reported in our previous publications (Xiao et al., 2013; Yang, 2012; Yang et al., 2011).

4.2. Application in bubble columns of large diameters

To further verify the new inlet model for columns of large diameters, CFD simulation using the new inlet model is performed for the experimental system of Chen et al. (1999). Detail information is listed in Table 3.

In this case, to avoid the liquid overflow from the top of the column, the column height is extended to 3 m. The space above the column height of 0.89 m is defined as the fully-developed region of the flow in terms of the experiments of CARPT/CT measurements of Chen et al. (1999). Since the column was under batch-operated conditions, the static liquid height with zero gas holdup is filled up to 1.7 m. The rest part of the column is the liquid-free region.

Figs. 13 and 14 illustrate the time-averaged radial distribution of gas holdup and liquid axial velocity. For the simulation using the uniform inlet condition, the gas holdup profile appears to be rather flat and the gas holdup is over-predicted, and the liquid axial velocity is under-predicted at the centre, which suggests that the uniform inlet boundary is not adequate to fully reflect the flow characteristics in the large-diameter bubble column. For the simulation using the new inlet model, the radial distribution of gas holdup and liquid axial velocity is in better agreement with experimental data. The difference may be attributed to the velocity gradients caused by these two inlet models. The practical velocity gradient can be reasonably reflected in the new inlet model but neglected in the uniform inlet condition. In the latter case, additional radial force models may be required to recover the effects caused by the practical velocity gradient, e.g., tuning the lift coefficient.

In order to further test the new inlet model in the modelling of large-diameter bubble columns, the experimental system of Menzel et al. (1990) with a column diameter of 600 mm was simulated. The superficial gas velocity is 0.072 m/s. The simulation results of local gas holdup profiles along with the experiment data are illustrated in Fig. 15. The above two cases demonstrated that the new inlet model is also suitable for bubble columns with large diameters.

5. Conclusions

A new inlet model was proposed to approximate the effects caused by flow conditions and distributor geometries, and validated by the experiments in literature for the three bubble columns with diameters of 0.138 m, 0.44 m or 0.6 m. The simulation demonstrates that the uniform inlet boundary condition is inadequate in the prediction of both total and local gas holdup, in particular for higher gas flow rates, when the non-drag forces are not included in the simulation. The new inlet model is able to achieve the same level of accuracy as the hole case in which the full geometry of gas distributors is modelled. This is because the new inlet model can reasonably allocate the momentum onto the cross-section by the distribution functions proposed, and the effects of real geometries of distributors are considered as the parameters in the new inlet model. The new model is suitable for the simulation of both lab-scale and large size bubble column reactors, and able to reasonably predict the gas holdup profiles for different superficial gas velocities when the DBS drag model is used. The number of mesh cells can be reduced by approximately 10 times compared to the hole case, which is of practical significance for the simulation of industrial scale reactors.

Acknowledgements

The authors wish to thank the long-term support from National Natural Science Foundation of China (NSFC) (Grant nos. 91434121 and 91534118) and Ministry of Science and Technology of China (Grant no. 2013BAC12B01). Weibin Shi would also like to acknowledge the Ph.D. scholarship of the International Doctoral Innovation Centre (IDIC) of University of Nottingham Ningbo China and the support of EPSRC (Grant no. EP/G037345/1).

References

Akhtar, M.A., Tade, M.O., Pareek, V.K., 2006. Two-fluid Eulerian simulation of bubble column reactors with distributors. J. Chem. Eng. Jpn. 39, 831–841.
Bahadori, F., Rahimi, R., 2007. Simulations of gas distributors in the design of shallow bubble column reactors. Chem. Eng. Technol. 30, 443–447.
Bao, D., Zhang, X., Dong, H.F., Ouyang, Z.L., Zhang, X.P., Zhang, S.J., 2015. Numerical simulations of bubble behavior and mass transfer in CO_2 capture system with ionic liquids. Chem. Eng. Sci. 135, 76–88.
Behkish, A., Lemoine, R., Oukaci, R., Morsi, B.I., 2006. Novel correlations for gas holdup in large-scale slurry bubble column reactors operating under elevated pressures and temperatures. Chem. Eng. J. 115, 157–171.
Bordel, S., Mato, R., Villaverde, S., 2006. Modeling of the evolution with length of bubble size distributions in bubble columns. Chem. Eng. Sci. 61, 3663–3673.
Camarasa, E., Vial, C., Poncin, S., Wild, G., Midoux, N., Bouillard, J., 1999. Influence of coalescence behaviour of the liquid and of gas sparging on hydrodynamics and bubble characteristics in a bubble column. Chem. Eng. Process. 38, 329–344.
Chen, J.H., Yang, N., Ge, W., Li, J.H., 2009. Modeling of regime transition in bubble columns with stability condition. Ind. Eng. Chem. Res. 48, 290–301.
Chen, J.W., Li, F., Degaleesan, S., Gupta, P., Al-Dahhan, M.H., Dudukovic, M.P., Toseland, B.A., 1999. Fluid dynamic parameters in bubble columns with internals. Chem. Eng. Sci. 54, 2187–2197.
Chen, P., Dudukovic, M.P., Sanyal, J., 2005a. Three-dimensional simulation of bubble column flows with bubble coalescence and breakup. AIChE J. 51, 696–712.
Chen, P., Sanyal, J., Dudukovic, M.P., 2005b. Numerical simulation of bubble columns flows: effect of different breakup and coalescence closures. Chem. Eng. Sci. 60, 1085–1101.
Deckwer, W.D., 1992. Bubble Column Reactors. Wiley, Chichester, UK.
Deen, N.G., Solberg, T., Hjertager, B.H., 2000. Numerical simulation of gas–liquid flow in a square cross section bubble column, in: Proceedings of the 14th International congress of chemical and process engineering (CHISA), Praha, Czech Republic.
Deen, N.G., Solberg, T., Hjertager, B.H., 2001. Large eddy simulation of the gas-liquid flow in a square cross-sectioned bubble column. Chem. Eng. Sci. 56, 6341–6349.
Delnoij, E., Lammers, F.A., Kuipers, J.A.M., vanSwaaij, W.P.M., 1997. Dynamic simulation of dispersed gas-liquid two-phase flow using a discrete bubble model. Chem. Eng. Sci. 52, 1429–1458.
Dhotre, M.T., Joshi, J.B., 2007. Design of a gas distributor: three-dimensional CFD simulation of a coupled system consisting of a gas chamber and a bubble column. Chem. Eng. J. 125, 149–163.
Guan, X.P., Gao, Y.X., Tian, Z., Wang, L.J., Cheng, Y.W., Li, X., 2015. Hydrodynamics in bubble columns with pin-fin tube internals. Chem. Eng. Res. Des. 102, 196–206.
Haque, M.W., Nigam, K.D.P., Joshi, J.B., 1986. Optimum gas sparger design for bubble-columns with a low height-to-diameter ratio. Chem. Eng. J. Biochem. Eng. J. 33, 63–69.
Hills, J.H., 1974. Radial nonuniformity of velocity and voidage in a bubble column. Trans. Inst. Chem. Eng. 52, 1–9.
Hunt, J.C.R., Auton, T.R., Sene, K., Thomas, N.H., Kowe, R., 1987. ICHMT Int Seminar on Transient Phenomena in Multiphase Flow., Dubrovnik, Yugoslavia, pp. 103–125.
Krishna, R., van Baten, J.M., 2001. Eulerian simulations of bubble columns operating at elevated pressures in the churn turbulent flow regime. Chem. Eng. Sci. 56,

6249–6258.
Laborde-Boutet, C., Larachi, F., Dromard, N., Delsart, O., Schweich, D., 2009. CFD simulation of bubble column flows: investigations on turbulence models in RANS approach. Chem. Eng. Sci. 64, 4399–4413.
Larachi, F., Desvigne, D., Donnat, L., Schweich, D., 2006. Simulating the effects of liquid circulation in bubble columns with internals. Chem. Eng. Sci. 61, 4195–4206.
Li, G., Yang, X.G., Dai, G., 2009. CFD simulation of effects of the configuration of gas distributors on gas-liquid flow and mixing in a bubble column. Chem. Eng. Sci. 64, 5104–5116.
Li, W.L., Zhong, W.Q., 2015. CFD simulation of hydrodynamics of gas-liquid-solid three-phase bubble column. Powder Technol. 286, 766–788.
Lucas, D., Tomiyama, A., 2011. On the role of the lateral lift force in poly-dispersed bubbly flows. Int. J. Multiph. Flow. 37, 1178–1190.
Lucas, D., Prasser, H.M., Manera, A., 2005. Influence of the lift force on the stability of a bubble column. Chem. Eng. Sci. 60, 3609–3619.
Lucas, D., Rzehak, R., Krepper, E., Ziegenhein, T., Liao, Y., Kriebitzsch, S., Apanasevich, P., 2016. A strategy for the qualification of multi-fluid approaches for nuclear reactor safety. Nucl. Eng. Des. 299, 2–11.
Masood, R.M.A., Rauh, C., Delgado, A., 2014. CFD simulation of bubble column flows: an explicit algebraic Reynolds stress model approach. Int. J. Multiph. Flow 66, 11–25.
Menzel, T., Weide, T.I.D., Staudacher, O., Wein, O., Onken, U., 1990. Reynolds shear-stress for modeling of bubble column reactors. Ind. Eng. Chem. Res. 29, 988–994.
Mudde, R.F., Harteveld, W.K., van den Akker, H.E.A., 2009. Uniform flow in bubble columns. Ind. Eng. Chem. Res. 48, 148–158.
Rampure, M.R., Kulkarni, A.A., Ranade, V.V., 2007. Hydrodynamics of bubble column reactors at high gas velocity: experiments and computational fluid dynamics (CFD) Simulations. Ind. Eng. Chem. Res. 46, 8431–8447.
Rampure, M.R., Mahajani, S.M., Ranade, V.V., 2009. CFD simulation of bubble columns: modeling of nonuniform gas distribution at sparger. Ind. Eng. Chem. Res. 48, 8186–8192.
Ranade, V.V., Tayalia, Y., 2001. Modelling of fluid dynamics and mixing in shallow bubble column reactors: influence of sparger design. Chem. Eng. Sci. 56, 1667–1675.
Rigopoulos, S., Jones, A., 2003. A hybrid CFD – reaction engineering framework for multiphase reactor modelling: basic concept and application to bubble column reactors. Chem. Eng. Sci. 58, 3077–3089.
Sankaranarayanan, K., Sundaresan, S., 2002. Lift force in bubbly suspensions. Chem. Eng. Sci. 57, 3521–3542.
Sokolichin, A., Eigenberger, G., 1999. Applicability of the standard k-epsilon turbulence model to the dynamic simulation of bubble columns: part I. Detailed numerical simulations. Chem. Eng. Sci. 54, 2273–2284.
Sokolichin, A., Eigenberger, G., Lapin, A., 2004. Simulation of buoyancy driven bubbly flow: established simplifications and open questions. AIChE J. 50, 24–45.
Tabib, M.V., Roy, S.A., Joshi, J.B., 2008. CFD simulation of bubble column - An analysis of interphase forces and turbulence models. Chem. Eng. J. 139, 589–614.
Tomiyama, A., 1998. Struggle with computational bubble dynamics. Multiph. Sci. Technol. 10 (4), 369–405.
Troshko, A.A., Zdravistch, F., 2009. CFD modeling of slurry bubble column reactors for Fisher-Tropsch synthesis. Chem. Eng. Sci. 64, 892–903.
Van Baten, J.M., Krishna, R., 2004. Scale effects on the hydrodynamics of bubble columns operating in the heterogeneous flow regime. Chem. Eng. Res. Des. 82, 1043–1053.
Wang, T.F., Wang, J.F., Jin, Y., 2006. A CFD-PBM coupled model for gas-liquid flows. AlChE J. 52, 125–140.
Wang, Q.G., Yao, W., 2016. Computation and validation of the interphase force models for bubbly flow. Int. J. Heat Mass Transfer 98, 799–813.
Wiemann, D., Mewes, D., 2005. Calculation of flow fields in two and three-phase bubble columns considering mass transfer. Chem. Eng. Sci. 60, 6085–6093.
Xiao, Q., Yang, N., Li, J., 2013. Stability-constrained multi-fluid CFD models for gas–liquid flow in bubble columns. Chem. Eng. Sci. 100, 279–292.
Yang, N., 2012. A multi-scale framework for CFD modelling of multi-phase complex systems based on the EMMS approach. Prog. Comput. Fluid Dyn. 12, 220–229.
Yang, N., Chen, J.H., Zhao, H., Ge, W., Li, J.H., 2007. Explorations on the multi-scale flow structure and stability condition in bubble columns. Chem. Eng. Sci. 62, 6978–6991.
Yang, N., Wu, Z.Y., Chen, J.H., Wang, Y.H., Li, J.H., 2011. Multi-scale analysis of gas-liquid interaction and CFD simulation of gas-liquid flow in bubble columns. Chem. Eng. Sci. 66, 3212–3222.
Zhang, D., Deen, N.G., Kuipers, J.A.M., 2006. Numerical simulation of the dynamic flow behavior in a bubble column: a study of closures for turbulence and interface forces. Chem. Eng. Sci. 61, 7593–7608.
Ziegenhein, T., Rzehak, R., Krepper, E., Lucas, D., 2013. Numerical simulation of polydispersed flow in bubble columns with the inhomogeneous multi-size-group model. Chem. Ing. Tech. 85, 1080–1091.